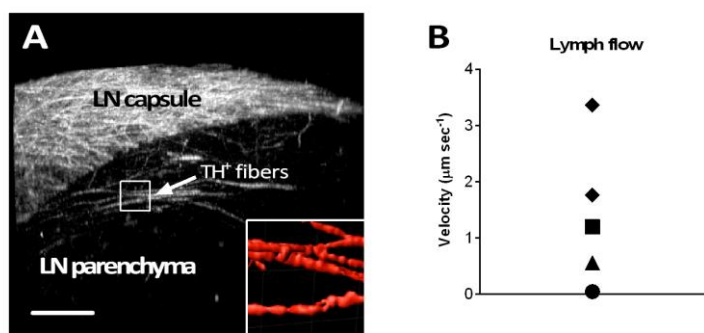
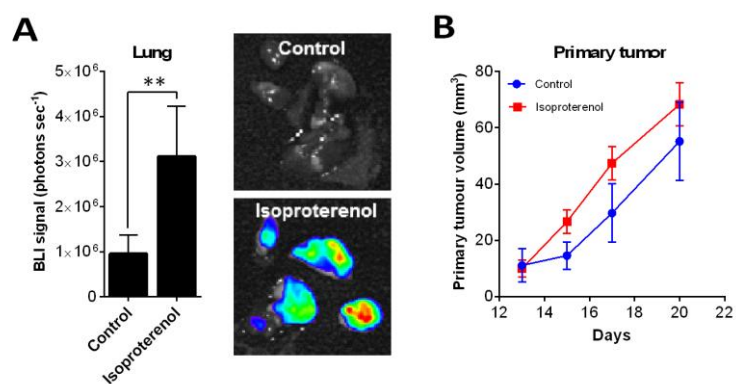


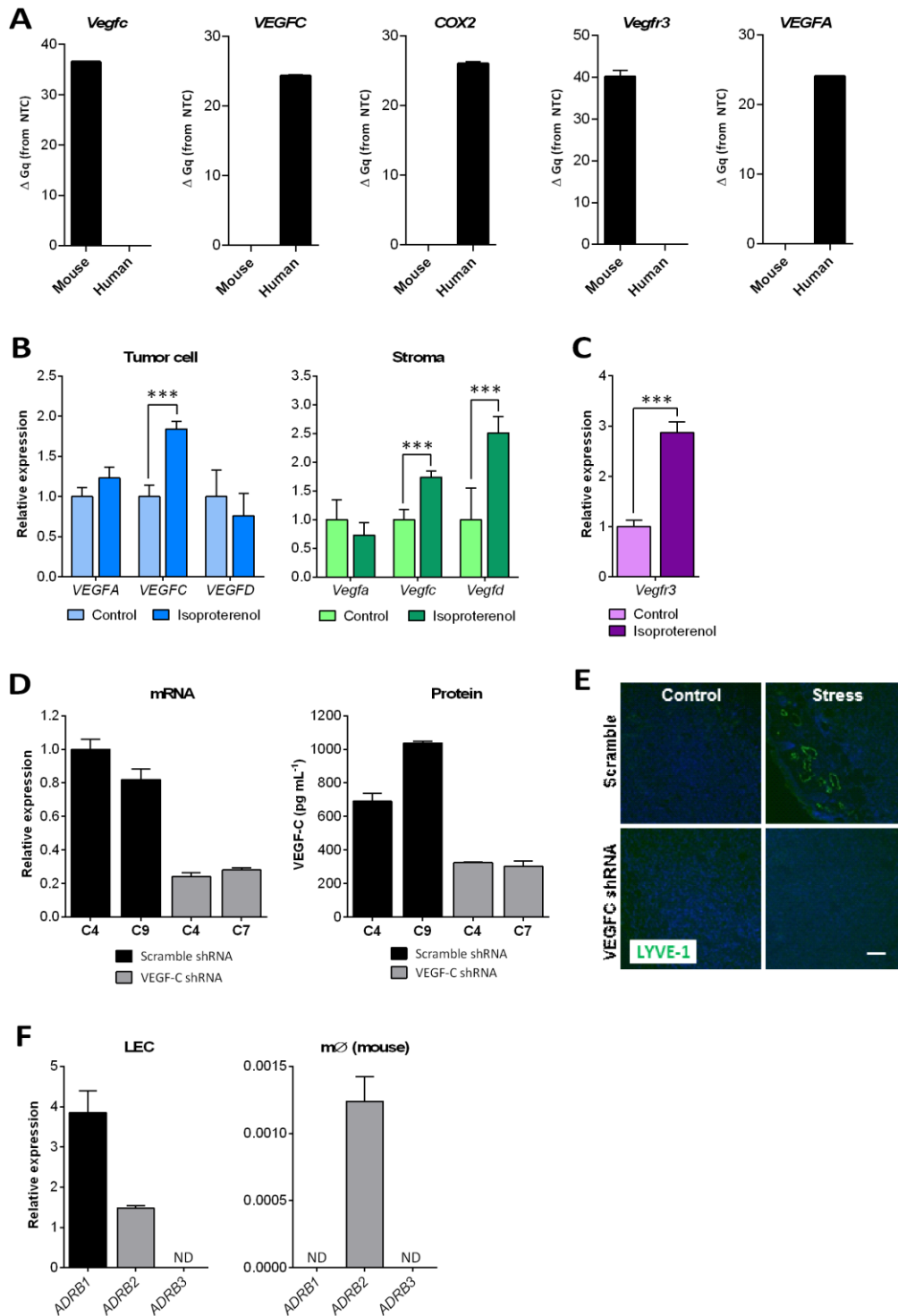
**Supplementary Figure 1. Chronic stress remodels tumor lymphatic architecture** (A) Representative image of LYVE-1<sup>+</sup> vessel staining (inset) in topographical relation to the tumor edge (dashed line). Scale bar: 100  $\mu$ m (inset; 20  $\mu$ m). (B) Mass of MDA-MB-231 primary mammary tumors of control versus stressed mice (n = 5). N.S. = not significant. (C) Quantification of LVD (LYVE-1<sup>+</sup>, green) and representative immunostaining in 66cl4 primary tumors of control or stressed mice. Blue: nuclear staining. Data represent mean of >8 fields of view (n = 5). (D) Correlation of lymphatic vessel diameter against blood vessel diameter. (E) Cell embolus (asterisk) in LYVE-1<sup>+</sup> (red) lymphatic vessel. Blue: nuclear staining. Scale bar: 200  $\mu$ m. (F) Top: Representative fluorescent image of collecting lymphatic vessel (LV) containing mCherry-tagged MDA-MB-231 tumor cells (orange) and adjacent autofluorescent blood capillary (BC) and blood vessel (BV). Bottom: Cross-sectional view of a maximum intensity projection of the multiphoton image. Tumor cells: red. (G) Quantification of bioluminescence imaging in control versus stressed mice with MDA-MB-231 tumors up to 18 days after tumor cell (n = 5 at each timepoint). (H) Frequency of tumor-cell positive lymph nodes (LN) in control versus stressed mice (n = 13). All data represent mean  $\pm$  SE. \* p < 0.05, \*\*p < 0.01, \*\*\*p < 0.001 by Student's t-test.



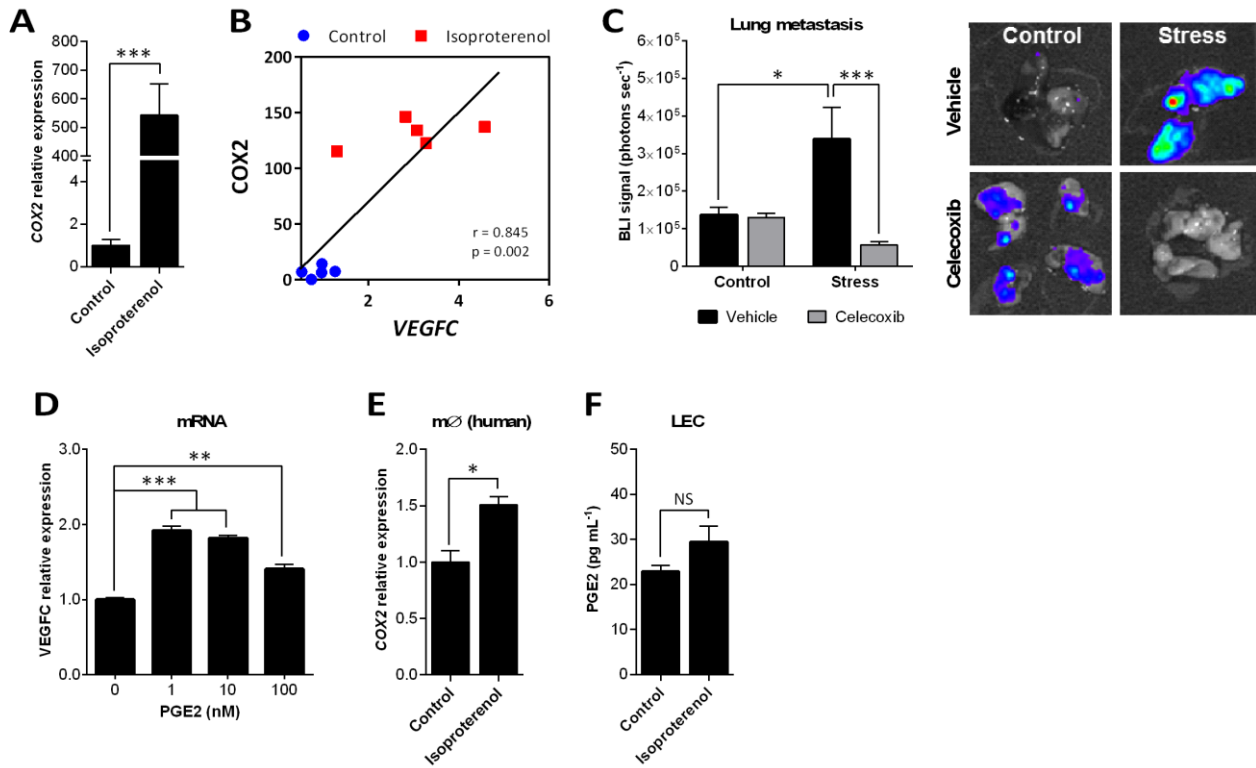
**Supplementary Figure 2. Lymph node innervation and measurement of lymphatic flow (A)** Multi-photon image of a lymph node innervated by TH<sup>+</sup> sympathetic nerve fibers from a C57Bl/6-TH-mCherry mouse. The arrow indicates the location of TH<sup>+</sup> fibers within the lymph node parenchyma and dense innervation of the lymph node (LN) capsule. Scale bar: 100  $\mu\text{m}$ . The inset represents a space filling model showing varicosities that release NE. Scale: 20  $\mu\text{m}$ . **(B)** Quantification of baseline lymph velocity in BALB/c *nu/nu* mice ( $n = 5$ ).



**Supplementary Figure 3. Beta-adrenergic signaling increases metastasis (A)** Representative images of lung metastasis and quantification of lung bioluminescence in control or isoproterenol treated mice ( $n = 5$ ).  $**p < 0.01$  by Student's t-test. **(B)** Primary mammary tumor volume of control or isoproterenol treated mice over time. Data represent mean  $\pm$  SE ( $n = 5$  at each timepoint).



**Supplementary Figure 4. VEGFC mediates stress-induced lymphatic remodeling** (A) Specificity of PCR probes against 66cl4 (mouse) and MDA-MB-231 (human) cells. (B) qRT-PCR analysis of human-specific (tumor cell) and mouse-specific (stromal) lymphangiogenesis-linked gene expression in MDA-MB-231 primary tumors (n = 5). (C) qRT-PCR analysis of mouse-specific *Vegfr3* (*Flt4*) gene expression in MDA-MB-231 primary tumors (n = 5). (D) Quantitative analysis of *VEGFC* gene expression (left) and protein levels (right) in MDA-MB-231 clones treated with scramble (SCR) or *VEGFC* (KD) shRNA (n = 3). (E) Representative LYVE-1 (green) and nuclear (blue) staining of MDA-MB-231 tumors expressing scramble or *VEGFC* shRNA. Scale bar: 100  $\mu$ m. (F) qRT-PCR analysis of *ADRB1*, -2 and -3 gene expression in human lymphatic endothelial cells (LECs) and primary mouse bone-marrow derived macrophages. ND = not detected. (n = 3). All data represent the mean  $\pm$  SE. \*p < 0.05 and \*\*\*p < 0.001 by two-way ANOVA on log transformed data (*post hoc* Tukey's adjustment) or Student's t-test.



**Supplementary Figure 5. Stress remodels tumor lymphatics via inflammation** (A) qRT-PCR analysis of *COX2* gene expression in CD11b<sup>+</sup>F4/80<sup>+</sup> tumor-associated macrophages (TAMs) isolated from 66cl4 tumors from mice treated with vehicle or isoproterenol ( $n = 3$ ). (B) Quantitative analysis of relationship between *COX2* and *VEGFC* expression in MDA-MB-231 tumors of control or isoproterenol-treated mice. Pearson coefficient 0.845 ( $p = 0.002$ ,  $n = 5$ ) (C) *Ex vivo* quantification and representative bioluminescence images of lung metastasis at day 22 of MDA-MB-231 tumor progression from celecoxib treated control or stressed mice ( $n = 5$ ). (D) qRT-PCR analysis of *VEGFC* gene expression in MDA-MB-231 cells treated with increasing concentrations of PGE2. ( $n = 3$ ). (E) qRT-PCR analysis of *COX2* gene expression in U937 monocyte-derived macrophages in response to vehicle or isoproterenol ( $n = 3$ ). (F) PGE2 production in lymphatic endothelial cells (LECs) treated with vehicle or isoproterenol *in vitro* measured by ELISA. All data represent mean  $\pm$  SE. \* $p < 0.05$ , \*\* $p < 0.01$  and \*\*\* $p < 0.001$  by Two-way ANOVA test (*post hoc* Tukey's adjustment) or Student's t-test.

## Supplementary Tables

	Mean coefficients ( $\mu_i$ )	Dispersion coefficients ( $\Phi_i$ )
Intercept	-4.75(0.30)*	3.48(0.35)*
Stress	0.86(0.42)*	-0.97(0.48)*
Control + Propranolol	0.13(0.44)	-0.20(0.50)
Stress + Propranolol	0.66(0.43)	0.71(0.49)

**Supplementary Table 1. Estimated coefficients for the beta regression model of the effect of stress and BB (propranolol) on LYVE-1 immunostaining.** Beta ( $\mu_i$ ,  $\Phi_i$ ) where  $\mu_i$  is the mean LVD, and  $\mu_i(1-\mu_i)/\Phi_i$  is the variance in LVD across individual primary tumor sections. Both  $\mu_i$  and  $\Phi_i$  are modeled as linear combinations of the treatment effects. Estimates are obtained by maximum likelihood estimation. Standard errors are reported in parenthesis and with (\*) denoting that the coefficient is significantly different from 0 at the 5% significance level using a Z-test.

	LN positive	LN negative	TOTAL
Control	8	18	26
Stress	15	11	26
TOTAL	23	29	52

**Supplementary Table 2. Tumor cell positive lymph node status in control versus stressed mice.** Significance of association between stress and lymph node (LN) positivity for tumor cells.  $p = 0.093$  determined using Fisher's exact test.